ICES Journal of Marine Science

Long-term exposure to elevated pCO$_2$ more than warming modifies early-life shell growth in a temperate gastropod

Saskia Rühl,[1,2]* Piero Calosi,[2,3] Sarah Faulwetter,[4] Kleoniki Keklikoglou,[4] Stephen Widdicombe,[1] and Ana M. Queirós[1]

[1]Plymouth Marine Laboratory, Prospect Place, West Hoe, Plymouth PL1 3DH, UK
[2]Marine Biology and Ecology Research Centre, School of Marine Science and Engineering, Davy Building, Plymouth University, Drake Circus, Devon, Plymouth PL4 8AA, UK
[3]Département de Biologie, Chimie et Géographie, Université du Québec à Rimouski, 300 Allée des Ursulines, Rimouski, QC G5L 3A1, Canada
[4]Institute of Marine Biology, Biotechnology and Aquaculture, Hellenic Centre for Marine Resarch, Thalassocosmos, Heraklion, Crete 71500, Greece

*Corresponding author: tel: +7932529890; fax: +44 1752 633 101; e-mail: sru@pml.ac.uk

Co-occurring global change drivers, such as ocean warming and acidification, can have large impacts on the behaviour, physiology, and health of marine organisms. However, whilst early-life stages are thought to be most sensitive to these impacts, little is known about the individual level processes by which such impacts take place. Here, using mesocosm experiments simulating ocean warming (OW) and ocean acidification (OA) conditions expected for the NE Atlantic region by 2100 using a variety of treatments of elevated pCO$_2$ and temperature. We investigated their impacts on bio-mineralization, microstructure, and ontogeny of *Nucella lapillus* (L.) juveniles, a common gastropod predator that exerts important top-down controls on biodiversity patterns in temperate rocky shores. The shell of juveniles hatched in mesocosms during a 14 month long experiment were analysed using micro-CT scanning, 3D geometric morphometrics, and scanning-electron microscopy. Elevated temperature and age determined shell density, length, width, thickness, elemental chemistry, shape, and shell surface damages. However, co-occurring elevated pCO$_2$ modified the impacts of elevated temperature, in line with expected changes in carbonate chemistry driven by temperature. Young *N. lapillus* from acidified treatments had weaker shells and were therefore expected to be more vulnerable to predation and environmental pressures such as wave action. However, in some instances, the effects of both higher CO$_2$ content and elevated temperature appeared to have reversed as the individuals aged. This study suggests that compensatory development may therefore occur, and that expected increases in juvenile mortality under OA and OW may be counteracted, to some degree, by high plasticity in shell formation in this species. This feature may prove advantageous for *N. lapillus* community dynamics in near-future conditions.

Keywords: Climate change, CT scanning, early-life stage, electron microscopy, Juvenile, Mollusc, ocean acidification, ocean warming.

Introduction

Many marine organisms have evolved external shells that provide protection against predation, desiccation and other inhospitable abiotic factors, and prevent parasitism (Brusca and Brusca, 2003). A damage or loss of shell-mass therefore diminishes the organism's likelihood of survival (Parker *et al.*, 2013). Marine external shells are most frequently composed of a number of carbonated

forms including minerals such as calcium and magnesium, as well as organic coatings (Vermeij, 1995).

Calcium carbonate (CaCO$_3$) is the most common material in marine shells and can occur in several forms with different chemical and mechanical properties (Weiss *et al.*, 2002). Shell CaCO$_3$ composites are arranged in layers of varying complexity, each consisting of a different form of CaCO$_3$ (Falini *et al.*, 1996).

Aragonite and calcite are the two most common CaCO$_3$ forms (Suzuki and Nagasawa, 2013). Calcite is more structurally diverse and more stable but requires comparatively more time and energy to be produced than aragonite (Weiss et al., 2002). Calcite is also mechanically weaker, and more resistant to corrosive effects of low pH environments than aragonite, typically forming trigonal-rhombohedrally shaped crystals, (Weiss et al., 2002). Conversely, aragonite occurs in orthorhombic acicular crystals, often appearing in parallel layers. Both materials vary in seawater solubility according to variations in ocean carbonate chemistry and temperature (Plummer and Busenberg, 1982,). For instance, CO$_2$ driven acidification can cause reductions in CaCO$_3$ saturation, making calcification more energetically costly for individuals relying on aragonite and calcite (Feely et al., 2004). Under-saturation of CaCO$_3$ therefore increases the risk of fast rates of shell dissolution, at which recovery may not take place (Nienhuis et al., 2010). In addition, seawater magnesium carbonate (MgCO$_3$) may also become under-saturated because of carbonate chemistry changes in seawater. The magnesium: calcium (Mg^{2+}:Ca^{2+}) ratio in seawater influences organic calcification processes on a microscopic level, so acidification can tip calcification towards the deposition of specific forms (Ries, 2010). Low levels of Mg^{2+} favour the formation of calcite, and high levels favour the deposition of aragonite (Ries, 2010). Juvenile molluscs preferentially deposit aragonite, possibly due to weaker controls over the early biomineralisation processes (Weiss et al., 2002), and on approaching maturity, calcite deposition increases. Differences in mineralisation over the individual life cycle can therefore lead to higher mortality in juveniles due to predation or parasitism, because shells are not yet as stable nor as thick as in adults. These shells are also thought to dissolve more easily in conditions of lowered pH, especially in or just after the settling process (Green et al., 2004). Such conditions have been found increasingly often in marine environments around the world as a consequence of global climate change.

Changes in seawater temperature (i.e. ocean warming, "OW") and in carbonate chemistry and pH driven by increasing CO$_2$ emissions (i.e. ocean acidification, "OA") (IPCC 2014) are known to impact the integrity and morphology of the shell of adult marine organisms (Nienhuis et al., 2010; Thomsen et al., 2010; Melatunan et al., 2013). Some defence mechanisms such as decreased shell growth rates to preserve energy (Findlay et al., 2010) and increased calcification in a range of calcifying species across taxa have been observed in acidified conditions (Ries et al., 2009). However, whilst we have a good understanding of OW and OA impacts on adult shell bearing organisms, our current understanding of how the same stressors and their interactions may impact embryos and juveniles is still limited (Byrne and Przesllawski, 2013; Kurihara, 2008; Melatunan et al., 2013; Sanford et al., 2014). The energetic implications of dealing with multiple stressors can cause a reduction and/or reallocation of an organism's energy budget (Melzner et al., 2013) such that trade-offs among different homeostatic processes caused by a given stressor can reduce the individual's ability to cope with another stressor (e.g. Calosi et al., 2013). These interactions can lead to complex changes at the individual-level and in species interactions, affecting the natural structuring of biological communities (Queirós et al., 2015). As the survival of populations depends on the survival of their offspring (Widdicombe and Spicer, 2008), early-life stages (e.g. Dupont and Thorndyke, 2009), on transgenerational responses (e.g. Sunday et al., 2014) and species interactions are therefore

needed to scale up population and community level responses to climate change and OA (Reusch, 2014, Sunday et al., 2014).

This study aimed to quantify the combined effects of OW and OA as simulated through elevated CO$_2$ content and temperature treatments, on the shell development and growth of the juveniles of the temperate marine gastropod Nucella lapillus (Linnaeus, 1758), a predator that exerts important top-down controls on the biodiversity of North Atlantic temperate rocky shores (Trussel et al., 2003). Nucella lapillus (hereafter "N. lapillus") is an abundant species in temperate shores of the North Atlantic that exhibits a certain phenotypic plasticity in shell morphology and colour depending on latitude, microhabitat, physiological stress, and mechanical stresses such as those caused by wave actions and predation. N. lapillus is a direct developer that predates on habitat forming species such as barnacles and mussels, and has a great influence on benthic community structure and dynamics, habitat complexity, and diversity (Trussel et al., 2003; Sanford et al., 2014). In this study, shell length, width, thickness, density, crystallization, chemical make-up, and overall shapes of juveniles from different treatment combinations, at 3 and 9 weeks post hatching, were examined. Animals were collected over a 14 month mesocosm experiment featuring multiple combinations of elevated CO$_2$ content and temperature treatments (simulating various scenarios of OA and OW projected for the end to the 21st century in the region), during which marked effects of both stressors were observed in adult N. lapillus energetics and shell structure (Queirós et al., 2015). Considering that N. lapillus is a direct developer, we expected that if no phenotypic adjustment occurred during embryonic and post-hatching ontogeny, juveniles hatched during the experiment would develop shells with significant changes in growth patterns and chemistry, reflecting impacts observed in the parental lineage. However, if developmental acclimatisation was to occur, we expect no significant changes to be observed at the levels of shell, as phenotypic buffering could favour the maintenance of this ecologically and physiologically important structure.

Material and methods
Specimen acquisition
Juveniles of N. lapillus were collected during the NERC-DECC UK Ocean Acidification Research Programme's mesocosm experiments (Queirós et al., 2015), carried out at Plymouth Marine Laboratory's Intertidal Mesocosm Acidification System (PML-IMAS, Findlay et al., 2013) during 2011-2012. Mature individuals from a native population at Mouth Batten, Plymouth (N50° 21' 30.29", E-4° 7' 50.07") were collected and transferred to the PML-IMAS where they were exposed to five different treatments combining various temperature and pCO$_2$ levels for 14 months (Queirós et al., 2015). During the experiment, the offspring hatched from egg capsules laid in the mesocosm were maintained in this system, and analysed in the present study. A detailed description of the set-up, carbonate chemistry parameters and of how the experimental treatments were controlled can be found in Queirós et al. (2015). Briefly, five treatments combining seawater pCO$_2$ (380, 750 and 1000 ppm) at ambient temperature (A) and two pCO$_2$ treatments (380 and 750 ppm) at elevated temperature were simulated. These treatments are hereafter referred to as 380A, 750A and 1000A, and 380T and 750T, respectively. Ambient temperature was controlled to follow the seasonal cycle at the population source conditions (typically between 9 and

15 °C) and warming was simulated as a 2 °C offset above that variation (Queirós *et al.*, 2015). Throughout the experiment, egg capsules laid by adults in the treatment tanks were inspected on a weekly basis, and hatched juveniles varying between one and 14 weeks of age were recorded and collected for later analyses. Out of this collection, only those of 3 and 9 weeks of age were examined in the present study. The number of eggs and juveniles produced by the adults varied greatly between treatments, and in the 1000A treatment, only four individuals hatched in 14 months, possibly as the result of metabolic depression observed in adult *N. lapillus* (Queirós *et al.*, 2015). Due to the low replication level, this treatment group was therefore excluded from the current analysis. Twenty-four individuals from the other four (OA x OW) treatments were collected at random and analysed, three from each age group and treatment combination. All specimens were stored dry or in minimal amounts of distilled water at −80 °C before, in between and after analyses, and transported in liquid nitrogen where necessary.

Micro-CT scanning
Scanning was carried out at the Hellenic Centre of Marine Research (Crete, Greece). Each individual was inserted into an individual pipette tip which was sealed airtight and positioned upright in the scan chamber of a micro-tomograph (Skyscan 1172, Bruker, Belgium). The scan medium was always air, and no stains were used. Specimens were scanned with a voltage of 59 kV and a 167 µA current for the acquisition of morphological and density related data. Density measurement calibration was achieved experimentally and from past measurements of similar materials. The micro-tomograph has a maximum resolution of 4000 x 2672 pixels (∼0.8 µm *per* pixel). A filter with two layers of aluminium foil was used to minimize excess charge. These settings were optimized for the highest resolution (4,000x), an exposure time of 1915 ms and between 0.85 and 1.3 µm zoom, depending on the size of the specimen. Images were collected at full 360° rotation with no random movement, and averaging every two images at every rotation angle. Scanning parameters were recalibrated before each scan to ensure comparability between image sets (i.e. individuals).

Reconstruction of scanned specimens
The micro-CT projections were reconstructed into cross-sectional images of shells using a reconstruction software (NRecon, Skyscan, Bruker, Belgium), which is based on a modified Feldkamp's back-projection algorithm (Feldkamp *et al.*, 1984). This was accomplished as an automated function of the scanning process using graphics processor unit reconstruction (GPU recon). If specimens had inadvertently moved during image acquisition, the scan was repeated. Reconstructed scans of tilted specimens were straightened to achieve a uniform measure of length and width in 3D view (Dataviewer, Skyscan, Bruker, Belgium). Ten cross-sections of each shell (hereafter "slices") were reconstructed in pre-selected locations across the shell, which were standardized across individuals to optimize comparability between individual results (Figure 1).

Scan analysis and data extraction
Shell length, width, and thickness measurements were acquired using Dataviewer (Bruker, 2014). Shell thickness was averaged across the widest part of the shell (WP1) as well as the Mid-lip slice (ML1; Figure 1). A 15 pixel thick band was selected from the edge of the shell and inwards around the outside of each of the ten slices for density measurements, using the software Image J1.45S (National Institutes of Health, USA). This band ensured that the selected area had been in immediate contact with the external conditions and not protected by soft tissue or body fluids. Shell density was measured as the average 2D grey-scale pixel intensity using the whole band.

The visual comparison of shell surface damage between individuals was accomplished in a volume rendering software (CTVox, Skyscan, Bruker, Belgium), where a 3D visualization of the shells as image stacks was produced, manipulating factors such as opacity and lighting (Figure 2).

3D geometric morphometrics measurements
3D geometric morphometric methods were applied to the reconstructed 3D scans (i.e. shell plastic model, see Figure 2) to investigate potential changes in shell morphology associated with phenotypic plasticity responses. Due to limits on computer memory during processing, scan file size was reduced and, consequently, resolution also reduced by a factor of 16. This was achieved using the Dataviewer resizing option prior to reconstructing triangulated surfaces for each of the specimens using the software Amira (FEI, 2013). Surfaces were reconstructed using the 'SurfaceGen' option on the resampled dataset and the resulting models were saved in 'Polygon File Format' (.ply). Overall, the scans were reduced in size by a factor of ∼64, but only a low level of detail was lost post processing.

Surface models were then uploaded into software designed for the analysis and interpretation of three-dimensional shapes (Landmark editor, Wiley, 2007). Here, a series of type 1 and 2 landmarks were introduced in the form of single landmarks and curves (Figure 2) on the lip, on minimum and maximum points as well as on each end of and along the whorl.

By establishing this landmark protocol (Figure 2) in the first shell and reproducing it in the others through correspondence of each set of landmarks with those of the original specimen, comparable measures of shape could be applied to the distinct features shared by all shells. Data points were exported from Landmark into MorphoJ (Klingenberg, 2011) where models were adjusted in a procrustes fit: a forced adjustment of all involved models for the sake of comparability, before generating covariance matrices and conducting procrustes analyses. These measures were taken in order to achieve optimal shape alignment through scaling, rotation and translation of the models. Amira (FEI, 2013), the programme used to make the original 3D models, was also used to measure the volume of each of the specimen's shells.

Analysis of crystalline properties
At Plymouth University (Plymouth, UK), scanned specimens were positioned on the bottom of cylindrical moulds with the youngest shell part facing downwards and fixed in this position on a thin layer of generic superglue. The mould was filled with epoxy resin and left in a vacuum chamber to de-gas, until the shells were enclosed inside and outside by the resin. The encased specimens were left at 30 °C over night to allow the epoxy resin to harden before sanding and polishing the formerly lower surface off to the desired cross-section.
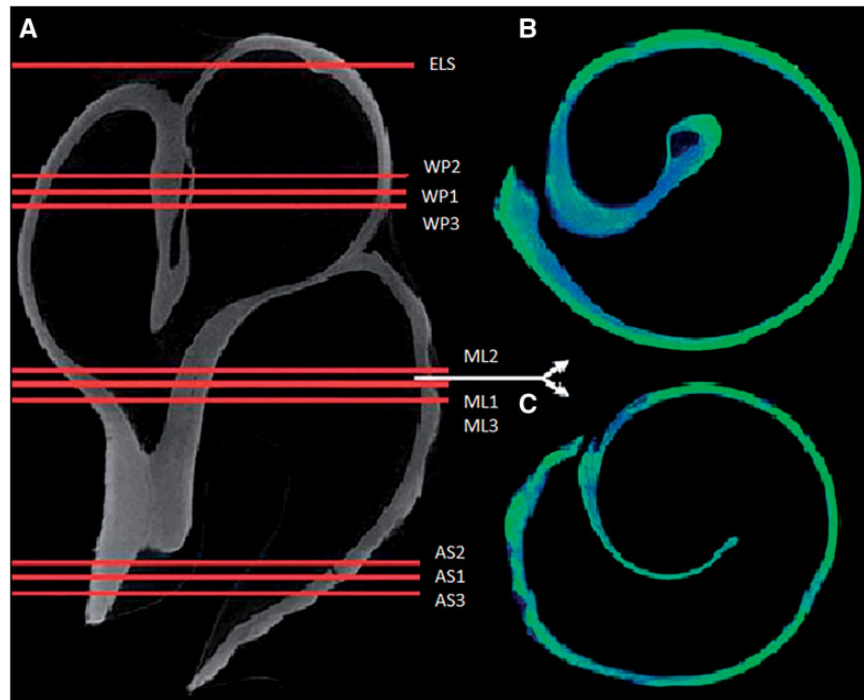
Figure 1. (a) Cross-sectional image of a 9 week old *Nucella* shell taken with the micro-CT scanner, indicating the position of the horizontal shell slices used for analysis. ELS = 3% from the top (posterior), AS1 = 3% from the bottom (anterior), AS2 = 4% from the bottom, AS3 = 5% from the bottom, WP1 = Widest Point, WP2 = WP1 + 1%, WP3 = WP1-1%, ML1 = Mid-Lip, ML2 = Mid-Lip +1%, ML3 = Mid-Lip -1%. Lighter grey indicates higher shell density, while black illustrates the background medium (air), not included in the analysis. 1 (b) and (c) are horizontal slices which illustrate the differences in density throughout two randomly selected 3 week old shells. (b) is a shell from ambient conditions (380 ppm CO_2/9–15 °C), while (c) was exposed to elevated temperatures and CO_2 input (750 ppm CO_2/9–15 +2 °C). Grey scale represents densities: lighter (green in online version): denser areas, darker (blue in online version): less dense areas. The scale bar below the vertically cross-sectioned shell equates to roughly 0.5 mm.
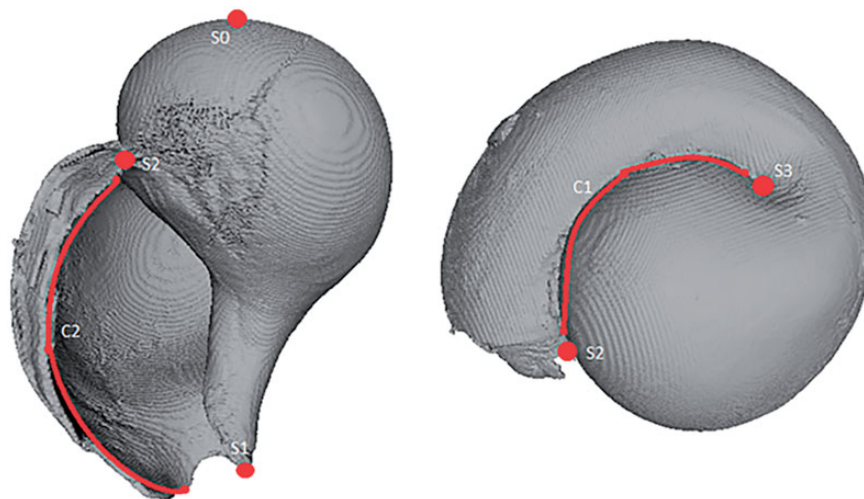

Figure 2. Surface model of a shell, reconstructed using µ-CT. The landmark protocol used in this study to evaluate shell morphology is represented by the annotated curves and dots. S0–S3 are single landmarks while C1 and C2 represent curves.

Hand polishing was carried out using first abrasive paper (P800 and P2500, FEPA P-grade), then 1 µm fine diamond paste on a bench-top sander (Kemet Int. Ltd., UK) with a fabric disc as foundation for the paste. Cross-sections were taken from comparable points in all shells. The surface of each cross-section was further etched with hydrochloric acid for 45 s to improve the exposure of a shell surface for visualization. Specimens were then carbon coated in a carbon sputter-coater (K450X, EmiTech, Quorum Technologies, UK) using carbon rods. Scanning electron microscopic energy dispersive x-ray analysis (JEOL JSM-6610 LV, JEOL, Tokyo, Japan) was used to determine the crystalline structure of each shell, and the relative thickness of homogenous and

crossed-lamellar layers were recorded, as possible. Where more than one crystal layer was present, x-ray spectra were selected from each of the cross-sections in the outermost layer of crystals to examine the most exposed regions. Images of each cross-section were taken for further analysis at appropriate magnification to determine crystal polymorph structure (Marxen *et al.*, 2008). The elemental ratio from each x-ray spectrum was recorded (for technique see Reed, 2005).

Statistical analysis

Shell weight, length, width, thickness, volume, and density data sets were analysed separately and differences between treatment and age groups investigated. All data were screened on whether they met the assumptions of a linear model by assessing independence of errors, homoscedasticity and normality of residuals. Where assumptions were met, Analysis of Variance (ANOVA; Fisher, 1925) was carried out for each response variable. Else, datasets we analysed using Generalized Least Squares (GLS; Cascetta, 1984) modelling, wherein the best fitting and most parsimonious models were selected, based on Akaike's Information Criterion (AIC; Akaike, 1973). The combined effects of temperature, pH and age on the similarity structures of the aggregated datasets (all response variables) were also investigated using crossed Analysis of Similarity (ANOSIM; Clarke, 1993) and the software Primer (Clarke and Gorley, 2014). This further step was undertaken to investigate whole-individual responses between treatments, allowing for consideration to be given to the potential variability in specific responses of individuals within treatment groups.

Additionally, similarity percentage tests (SIMPER; Clarke, 1993) were used to determine which variables most explained observed variation in the chemical make-up of the shells (i.e. elemental composition) between treatment and age groups. Statistical difference in chemical make-up of shells was tested between individuals as well as treatment- and age groups. Mean weights of each element within individual samples were then compared in Primer and R using crossed ANOSIM tests and GLS modelling. Out of all the elements (and element ratios) recorded in the spectral analysis, a special focus was put on analysing the magnesium:calcium ratios (Mg:Ca) because it is one of the factors determining crystallization within the shells. Non-metric Multi-Dimensional scaling (nMDS; Kruskal, 1964) was estimated based on Euclidean distances to explore overall dissimilarities between age and treatment groups. Unless otherwise specified, all data analyses were carried out in R (R foundation, Vienna).

Results

Shell surface

Shells of individuals exposed to elevated pCO_2 (i.e. 750 ppm, Figure 3) exhibited overall a greater proportion of rough textures and indentures on their surface than at ambient pCO_2, in both age groups, and this effect that was more pronounced under co-occuring elevated temperature conditions (750T cf. 380A). This can also be seen in the cross-sectional images in Figure 1, in which the shell exposed to high temperature and elevated pCO_2 (750T, Figure 1c) showed a distinctly more uneven surface than the control shell (380A, Figure 1b).

Shell micro-structure and chemistry

Shells' microstructures from individuals kept under control conditions (380A) exhibited a structure of separation into a neatly sorted crossed-lamellar (CL) inner layer of thin aragonitic $CaCO_3$ sheets and a thin, grainy homogenous (H) outer layer (Figure 4, 380A, 1-3). Shells of individuals kept under the elevated temperature condition (380T) exhibited similar structures but the thickness of the layers varied. Crossed-lamellar crystals varied in size and neatness of layering and the H layers were smoother than in the control treatment group (Figure 4, 380T, 1-3 cf. Figure 4, 380T). Shells kept at ambient temperature and elevated pCO_2 had lost the distinct layering and although both CL and H structures were recognisable, the transitional phase contained both (Figure 4, 750A, 1). The biggest change in shell microstructure however was found in 9 weeks old individuals exposed to high pCO_2 at ambient temperature and in shells of all ages where both temperature and pCO_2 had been increased. Here, the newest shell parts (closest to the growth edge at the lip) displayed a complete lack of layering with a new crystal structure that resembled neither CL nor H patterns found in other shells (Figure 4, 750T, 1-3).
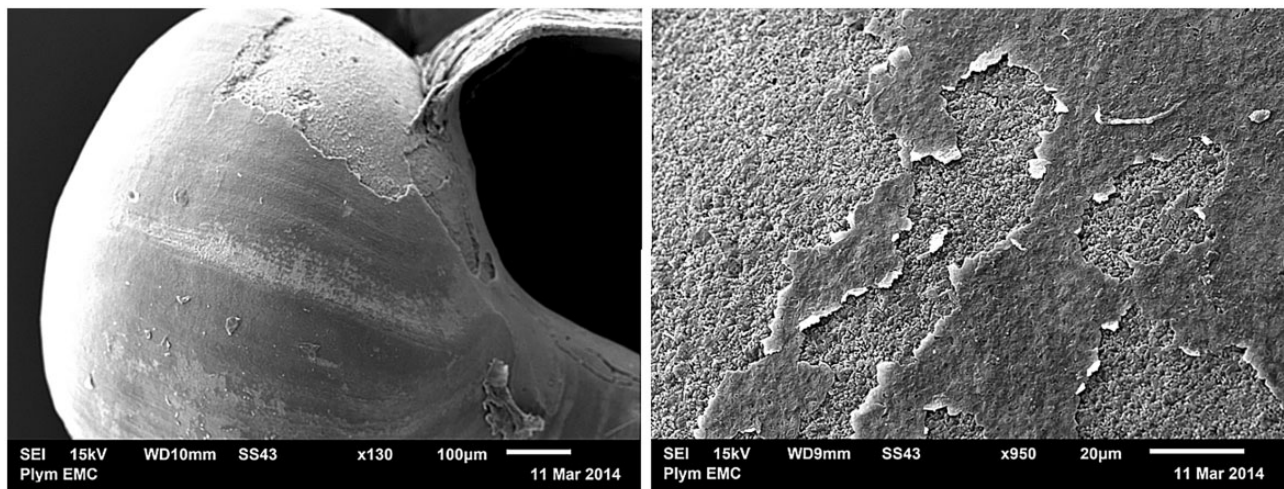

Figure 3. Images of shell exteriors taken with the electron microscope (EM) to show examples of surface damage in 750T (left) and 750A (right) shells.
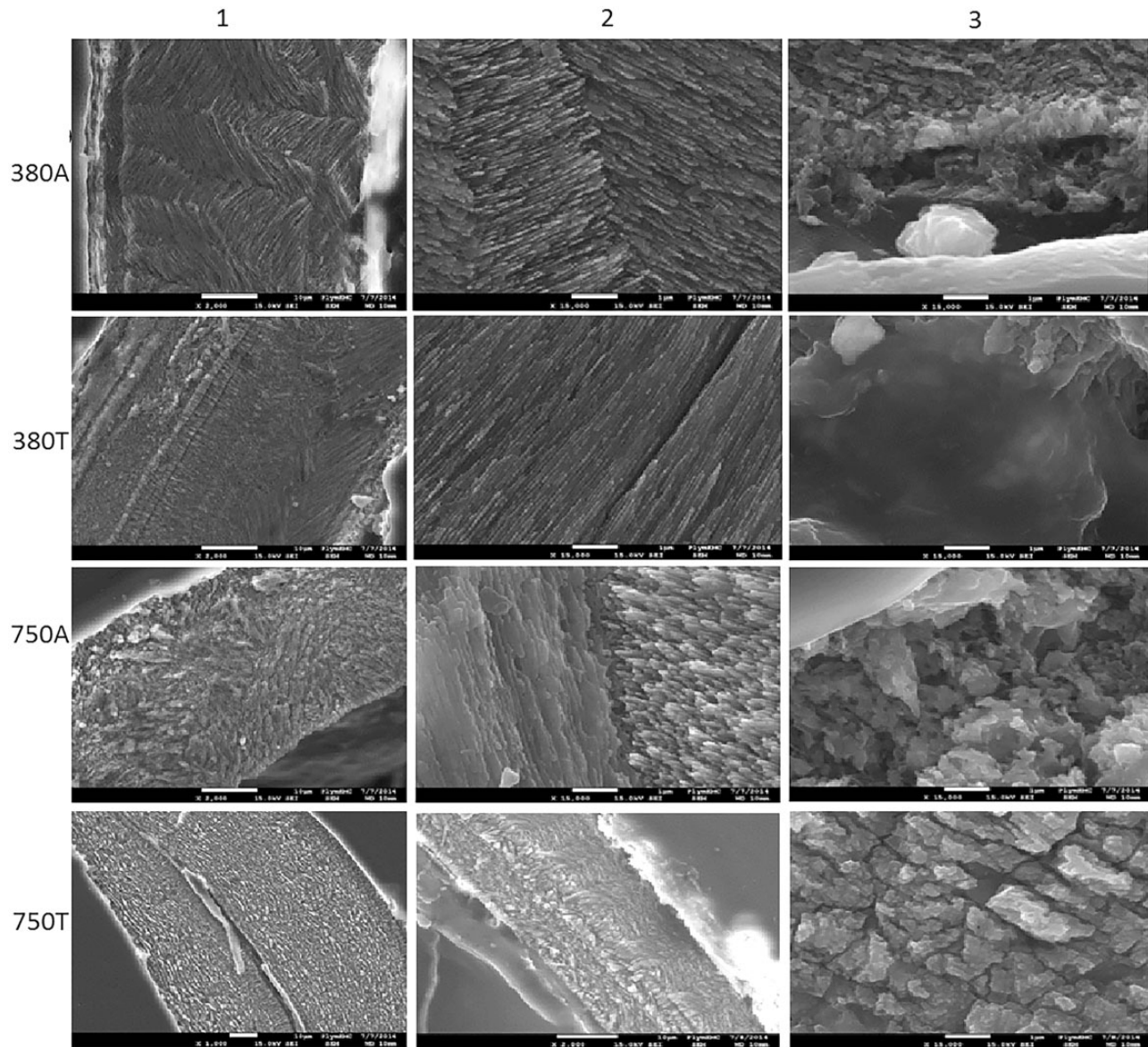
Figure 4. Electron microscopy images of the crystallized structures within shells of the older group in lines according to treatments; columns 1 represents a view of both layers together, 2 shows a close-up of the crossed-lamellar layer, and column 3 are images of the homogenous structures. The first picture depicting the 750T treatment represents a shell with no distinct difference between layers, the second in that line shows an example of a shell with remnants of crossed-lamellar structuring and the third picture is a close-up of the bark-like structure.

Although being most easily comparable to homogenous patterns, these new structures had eroded bark-like surfaces and little to no common direction of orientation of the crystals (Figure 4, 750T, 3). Some of the older parts of shells from elevated temperature and pCO_2 conditions displayed an unusually thin CL layer. The CL structures in those shells exhibited equally chaotically oriented crystals to what had been observed in 750A shells in both layers, and H structures more closely resembling the bark-like new structure than what had been recorded as H in 380A (Figure 4, 750T, 1). Crystal degeneration and deformation was stronger in the outermost parts of the shell than those closer to the columella.

The internal Mg:Ca ratio of the shells varied among individuals of different ages and exposures to different temperatures ($p < 0.05$, Figure 5a). Testing the other elements found within shells with SIMPER analyses confirmed variations in Ca^{2+} to be the greatest cause of dissimilarity between most sample groups, especially between pCO_2 treatments (65.7%) and age groups (65.1%). Variations between temperature groups were found to be due in equal parts to variation in oxygen, carbon, calcium, and magnesium proportions. The remaining deviations between age and CO_2 groups can be explained through variations in oxygen content, though all samples also contained traces of carbon and sodium.

Shell density

Shell density was found to be significantly lower in all experimental treatments when compared to individuals kept under control conditions. Exceptions to this pattern were 9 weeks old snails
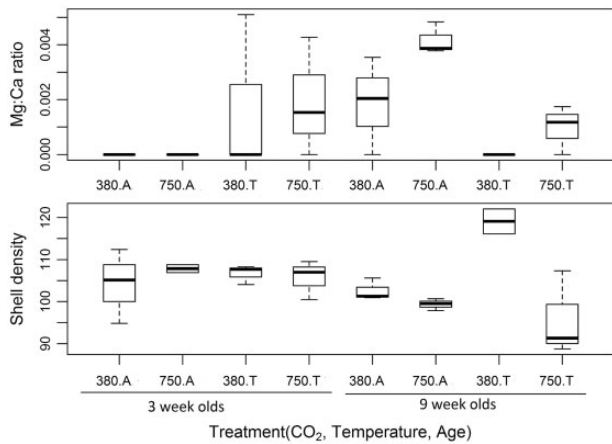
Figure 5. The effect of exposure to elevated pCO_2 and temperature, in juveniles of *N. lapillus* of different age (weeks 3 and week 9 post exposure) on shell (a) Mg^{2+}:Ca^{2+} ratios and (b) density which are coded along the x-axis with a combination of pCO_2 content (380 or 750 µatm), temperature (A for ambient, T for elevated by 2 °C) and age (3 and 9 weeks). Where the graph displays a Mg:Ca ratio of 0, this is due to 0 specimens having been available for this analysis from that treatment rather than a ratio of 0.

maintained at elevated temperature and pCO_2 treatment, which had the densest shells (750T). Exposure to elevated pCO_2 alone decreased shell density, but only in the 9 week old juveniles. The effects of age and temperature on shell density in isolation were less clear. The best GLS model included as main effects and interactions temperature, age and CO_2-content (Appendix 1, Supplementary Table S1, $p < 0.01$, Figure 5b).

Shell growth and shape

Groups of similar age and pCO_2 exhibited more variation shell morphology (i.e. length and shape) at ambient than at warm conditions, suggesting that temperature increased shell variability. The best GLS model for shell length included temperature, pCO_2 and age as main effects and interaction ($p < 0.01$, Appendix 1, Supplementary Table S2), suggesting that the effects of CO_2 and temperature on the shell lengths of *N. lapillus* differed with age (Figure 6a).

With regard to shell width, young shells of similar temperature groups treated at elevated pCO_2 levels (750A and 750T) were narrower than those treated in control pCO_2 conditions (380A and 380T), yet the opposite was true for old shells, which were wider at higher CO_2 (Figure 6b). Indeed, this effect was clear from the
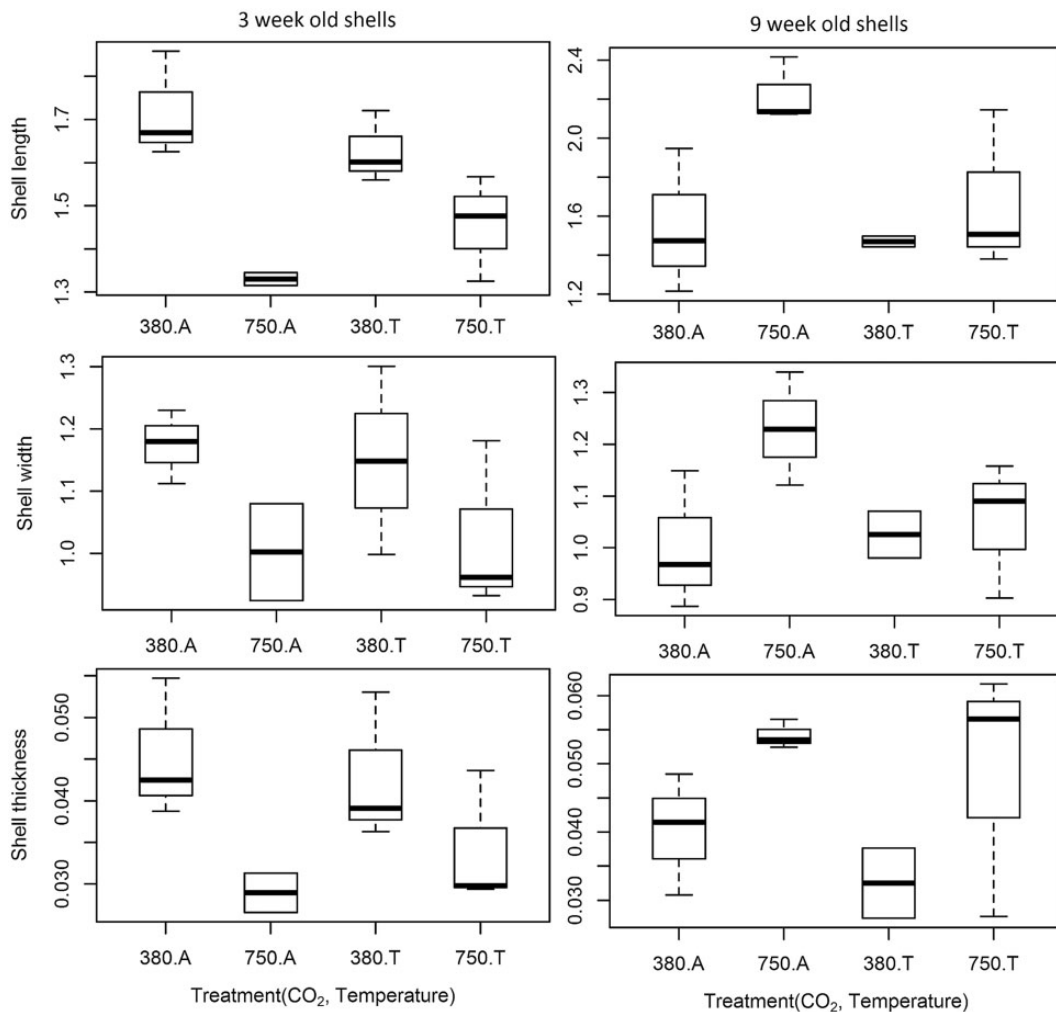

Figure 6. The effects of exposure to elevated pCO_2 and temperature, in juveniles of *N. lapillus* of different age (weeks 3 and 9 post exposure) on shell (a) length, (b) width and (c) thickness which are coded along the x-axis with a combination of CO_2 content (380 or 750), temperature (A for ambient, T for elevated) and age (3 and 9 weeks).

GLS analysis of shell width, for which the best GLS model included age and CO_2 as main effects and interaction, but not temperature ($p \leq 0.05$, Appendix 1, Supplementary Table S3).

Shell thickness

Similar to the patterns observed in other measurements, shells of young individuals exposed to similar temperature treatments were distinctly thinner when exposed to higher CO_2 concentrations, while older shells were thicker in high CO_2 (Figure 6c). The best GLS model included temperature, age, and CO_2 as main effects and interaction ($p < 0.05$, Appendix 1, Supplementary Table S4). Although temperature appeared to have an effect on shell thickness, this effect was variable across age and CO_2, and the effects of CO_2 and shell age were greater.

3D geometric morphometric shape analysis

As expected from the previous analyses, individuals variation in shell shape did not appear to be determined by any factor investigated in isolation, but was instead was explained by the combination of factors investigated, as represented by in the principle components ("PC") biplot (Figure 7). PC1-3 represented the majority of the variance in both the younger (73.17%, Figure 7b) and the older shells (77.22%, Figure 7a), representing mainly the angle and width of the shell whorl, aperture shape and length and the overall length, together creating the difference between narrower or wider shells. Whilst only a loose separation of the 750T individuals and those in the 380T treatment was apparent in the younger age group, PC2 (representing the shape of the whorl) clearly separated 750 ppm treatments (750A and 750T, positive PC score) from the 380 ppm treatments (380A and 380T, negative PC score) in the older age group. The latter likely reflects higher procrustes distances estimated for older shells, indicating that shell shape (as determined using landmark analysis) varied more in these the older than in the younger age group.

These results were confirmed by a two-way crossed ANOSIM analysis of externally measured data sets combined (length, width, density and thickness), which revealed that age (ANOSIM, global $R = 0.217$, $p < 0.05$) and CO_2 content (ANOSIM, global $R = 0.208$, $p < 0.05$) were the overall most deciding factors causing dissimilarities in shell variables. Differences in temperature, and the interaction of temperature with other factors however were not. All variables (lengths, width, density, and thickness) contributed roughly equal amounts of variation to the dissimilarities between groups ($\sim$20% each). Three-week old individuals were more similar to each other in shape (Figure 8), roughly clustering in the middle of the nMDS plot. Nine-week old individuals were distributed more widely around the edges of the plot, exhibiting greater variability in shape and in the relations between the different shape variables, and highlighting the role of treatments on shell development as time passed. The control group (380A) had the least within-group variation when compared with the others, with animals clustering in the centre of the nMDS
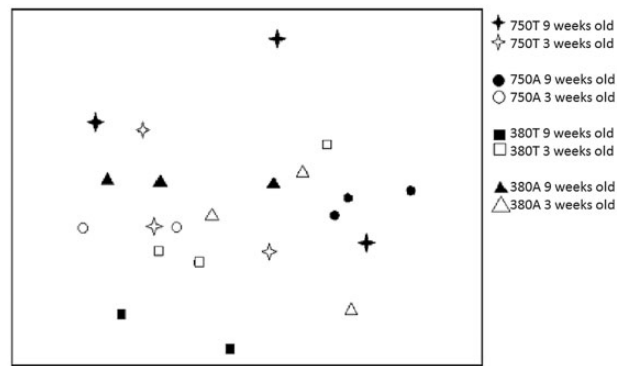

Figure 8. nMDS plot of similarities and dissimilarities between individuals according to age and treatment groups.
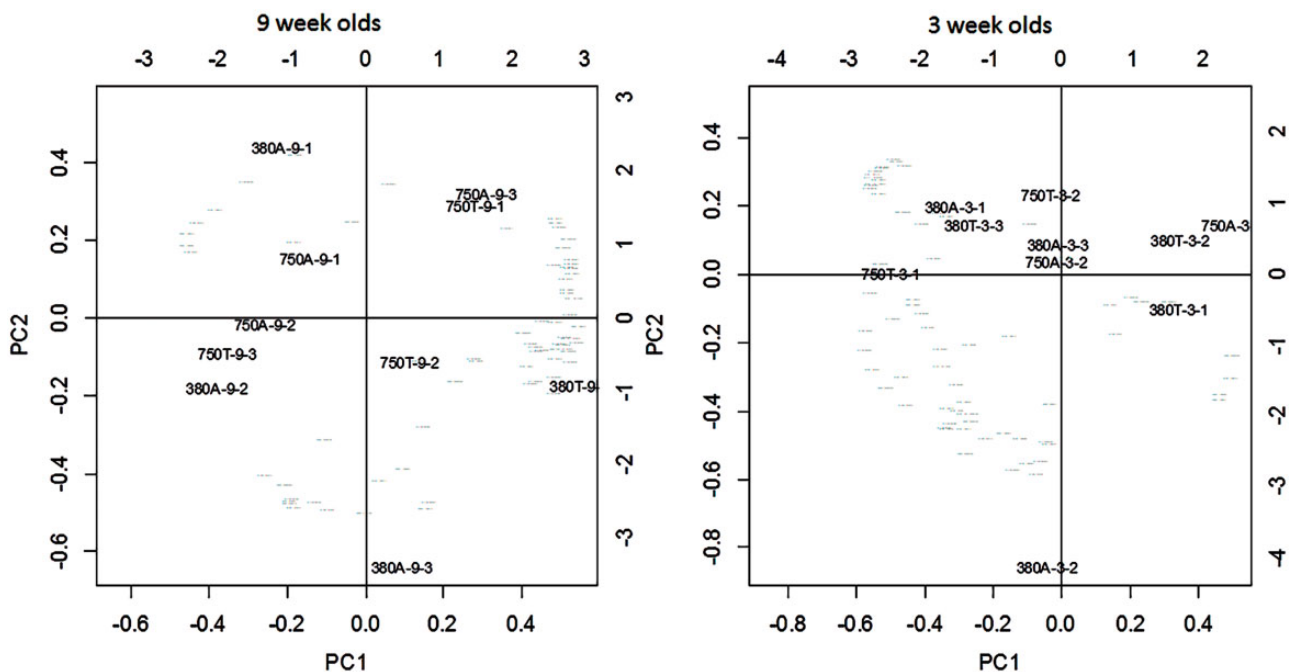

Figure 7. PC1 and PC2 of 9 week old shells to the left (a) and 3 weeks old shells to the right (b).

plot, while the most extreme 750T treatment led to greater dissimilarity in external shell characteristics.

Discussion

While the majority of structural shell features in juveniles of the gastropod *N. lapillus* appear to be influenced significantly by elevated pCO$_2$ and a two degree temperature offset on the temperature seasonal cycle, the impacts of these effects change as juveniles develop. Overall, the effects of CO$_2$ elevation and differences between age groups were evident, while higher temperatures appeared to act as a modifier of juveniles' responses to pCO$_2$. Differences in response between age groups may reflect how younger individuals are likely less capable to maintain their homeostasis and compensate for the increase in energy expenditure needed to upkeep shell structures. The differences observed between age groups may also likely reflect potential differences in parental investments in reproduction, given that the adults' metabolism and energy requirements were found to be significantly affected by exposure to both elevated pCO$_2$ and temperature during the 14-month mesocosm experiment (Queirós *et al.*, 2015). *N. lapillus* typically show a great deal of shell phenotypic plasticity when exposed to OA and OW conditions and our findings are in line with previous work showing shells' plastic responses to be more marked in individuals exposed to elevated temperature and pCO$_2$ conditions (Lardies *et al.*, 2014). This may be a consequence of individuals' physiological trade-offs (Turner *et al.*, 2015), here specifically between shell formation and repair vs. maintaining cellular metabolism and homeostasis. These findings are particularly relevant for *N. lapillus* ecology, because external shells provide a first barrier against predation, physiological and mechanical stress. Compensatory processes involved in shell deposition in *N. lapillus* may therefore prove beneficial under near future ocean conditions.

A significant reduction of shell growth and thickness after exposure to elevated pCO$_2$ has also been observed in other species (Barros *et al.*, 2013, Sanford *et al.*, 2014) and is thought to be linked to associated alteration of carbonate chemistry and growth inhibition in molluscs. Both of these effects make the organisms more vulnerable to crushing predators, such as crabs (Hughes and Elner, 1979) and might therefore lead to increased mortality rates in affected populations. It is unclear whether *N. lapillus* growth rates are affected by the higher CO$_2$ content directly, yet this study indicates that shell development was certainly modified. Importantly, and in contrast to previous studies, we found that as *N. lapillus* grew, older juveniles exhibited potentially compensatory responses. In older juveniles, shells were wider, longer and thicker under elevated pCO$_2$, potentially serving as a better defence. Despite evidence for increased surface damage and dissolution, potentially higher calcification rates may therefore in part have compensated for greater passive dissolution rates. This finding agrees with Melatunan *et al.* (2013) who, while focusing on adult gastropods, also found advantageous adaptations that allowed shell shape and size changes in molluscs affected by an offset in CO$_2$ content. Whether increased shell size is seen as adaptively advantageous overall is, however, not clear, because larger shells may attract greater risk of crab predation (Cotton *et al.*, 2004).

In general, gastropod shells are strengthened gradually through continuous calcification from within, leading to the thickening of the existing shell walls with age, as well as the establishing of a stronger microstructure in older shells (Weiss *et al.*, 2002). Mg:Ca ratios of calcifiers track the ratio of these minerals in seawater (Ries *et al.*, 2009). Concordantly, higher Mg:Ca ratios observed here in the shells of individuals exposed to elevated pCO$_2$ suggest that this elemental ratio increased in in those treatments. Higher Mg:Ca ratio in seawater is indeed known to favour the formation of Mg rich aragonite, instead of calcite (Ries *et al.*, 2009; Smith *et al.*, 2006), though seawater was not undersaturated for calcite or aragonite during our experiments (Queirós *et al.*, 2015, Supplementary Table S1). *N. lapillus* may therefore have a delayed transition from aragonite to calcite in more energetically challenging conditions (such as OA) as the former is less energetically demanding to deposit, particularly under in low pH scenarios (Weiss *et al.*, 2002). This mechanism could explain the wider, longer and thicker shells observed in the older juveniles from the high pCO$_2$ treatments in relation to the control, as though through this delay, more energy may have been available for the potentially increased calcification rate needed to address the greater shell damages observed in this treatment. Therefore, *N. lapillus* may have the ability to compensate, at least at this early stage of development, against the potential negative effects of carbonate chemistry conditions imposed by high CO$_2$ on shell deposition and dissolution. In line with recent findings (Fitzer *et al.*, 2016), the microstructure of the material deposited though this compensation exhibited a more chaotic CaCO$_3$ crystal formation. CaCO$_3$ microstructure strongly depends upon the presence of specific types of proteins in the extrapallial fluids (Bozhi, 2011). As these proteins are influenced by pH conditions (Thomsen *et al.*, 2010; Thompson *et al.*, 2000), organisms have been observed to alter crystallization patterns in high CO$_2$ conditions (Cusack *et al.*, 2007). The main shell building protein in *N. lapillus* is dermatopontin, which is 'acid soluble' (Suzuki and Nagasawa, 2013). Based on our results it is likely that even though these proteins are isolated from surrounding conditions, lower pH in the paleal fluid may have been present in individuals exposed to higher CO$_2$ contents, affecting the quality of crystallization within the shell. In some cases, proteins sensitive to low pH conditions can be substituted through the production of a range of different, less pH susceptible proteins (Hüning *et al.*, 2012), but this does not seem to be the case here.

The most important functions of complex shell structures are to provide structural support and protection from predator and physical stresses (e.g. wave action), which may cause the shell to crack or even break. The crossed-lamellar structures commonly found in the shell of healthy *N. lapillus* individuals prevent cracks in the shell from propagating through a constant change in crystal orientation (Suzuki and Nagasawa, 2013). Therefore, a thicker shell does not necessarily provide a better protection against predation if the cross-lamellar structure has disappeared, as we observed in the shells of juvenile snails exposed to elevated pCO$_2$, which were exacerbated by an elevation in temperature. Bark-like crystal shapes such as the ones found in the acidified samples in this study seem to be a phenomenon not yet widely described in the literature. Seeing as the current literature is still dominated by short-term single stressors studies of adult specimens, our results highlight the need to investigate the development of shell mineralogy and ultrastructure in juvenile molluscs under high temperature and CO$_2$ environments, over extended time periods, and considering the cumulative effects of exposure (such as here and in Dupont *et al.*, 2013). Adult individuals transplanted into conditions of elevated pCO$_2$ exhibit distinctly different calcification patterns in localized, newly built shell areas, including

unorganized crystals with varying growth directions (Hahn et al., 2011). However, the impact of high CO$_2$ content (and high temperatures) on shell physiology, as observed here, may still lead juveniles to higher vulnerability to predation and physical damage, despite the potential for adaptive processes taking place during shell deposition. Crystallization processes are similar in many organisms, even in far related groups, such as brachiopods, suggesting that the results from this study may be generalized to the impacts of similar conditions on the shell formation of juveniles of other species (Cusack et al., 2007).

Shell volume and weight were not impacted by exposure to elevated pCO$_2$ or temperature nor by the combination of the two factors, and surprisingly neither differed significantly among snails of different age classes in our experiment. Insignificant differences in shell volume may be due to the differences in shell shape we observed across treatments. A shape change may lead to shells that are more stout or narrow, consequentially changing shell size but not volume. Thicker shells in acidified treatments were also less dense (as seen in adult N. lapillus, Queirós et al., 2015), possibly explaining the lack of significant changes in shell weight. In our experiment, differences in shell shape were also not consistent across age groups, indicating that as Nucella grow, some compensatory responses seem to take place that affect its shape. Younger shells of both control pCO$_2$ treatments were most antithetic to one another while in the older groups it were shells from ambient pCO$_2$ combined with elevated temperature, as well as shells from elevated temperature combined with ambient temperature treatments. Gastropod morphology varies with environmental pressures such as predation, wave action and desiccation, substrate, CaCO$_3$ and O$_2$ concentration and temperature (Langerhans and Dewitt, 2002; Hollander et al., 2006; Queiroga et al., 2011). Although water chemistry, pH, and temperature have also been known to affect molluscs' shell shapes (Melatunan et al., 2013), the main factors influencing gastropods seem to be more of a more mechanical nature, namely predation and wave pressure (Queiroga et al., 2011; Langerhans and Dewitt, 2002). Shell slandering and squatting as seen in Guerra-Varela et al. (2009) prevents shells from being swept away by waves as well as making it harder for predators to crush them. The findings we observed here regarding shell shape further suggest that high CO$_2$ contents will potentially make young N. lapillus more vulnerable to both pressures, as shells became longer and stouter. Shells that are structurally weakened in this way are more likely to become easy prey to shell-crushing predators such as crabs (e.g. Melatunan et al., 2013). The shell variability we observed within treatment groups may be partly due to the fact that the embryonic development takes place within individual egg capsules which can lead to variations in size and developmental rate (Thorson, 1950). Differences in parental investment may also be a deciding factor of variability within age groups (Órdenes and Antonio, 2012). In this study, the duration of elevated pCO$_2$ and temperature exposure of the adults at the time of reproduction has not been taken into account because we could trace parental links within the experimental replicate, but this could have driven some of variation we observed within treatment groups that was not assignable to specific the treatments. This is a factor that should be considered in future studies.

The impact of elevated pCO$_2$ and temperature treatments on shell properties and growth pattern may lead to important implications for the size, shape, and structural integrity of shells in adult N. lapillus in a future ocean. We observed very little reproductive output in N. lapillus from our highest CO$_2$ treatment, though a congeneric Nucella species occurs and grows in natural vents (Selin, 2010), and as Nucella are direct developers, reliance on lateral input of individuals from adjacent areas seems unlikely. Survival and viable reproduction of N. lapillus therefore seems possible below or even up to 1000 ppm of CO$_2$, though the viability of offspring may be limited at this high level of pCO$_2$ (Queirós et al., 2015). At this most extreme pCO$_2$ level, expected in about a century according to projections reviewed by the IPPC (2014) in which seawater CO$_2$ may reach 1000 ppm, the combination of decreased investment in offspring by adults (4 juveniles born in 14 months, compared to 280 that were born in control conditions in the same time) and the observed impairment of the protective shell structures of juveniles leading to increased juvenile mortalities paint a bleak picture for Nucella in the near future ocean. Queirós et al. (2015) found that sea warming may counter-act metabolic depression caused by elevated pCO$_2$ in adult N. lapillus, and that decrease in prey acquisition due to limited chemo-sensory function under high CO$_2$ may be counteracted by adaptive predatory behaviour, in the absence of predators. However, weakened shell structures that make N. lapillus more vulnerable to predation may hinder the latter, both in adults and juveniles, as the observed altered predation behaviour requires more extensive foraging times and would therefore expose the individuals to predators for longer periods of time. It follows that, overall, Nucella lapillus, and other calcifiers with similar ecology are more likely to suffer from the effects of climate change and acidification than to benefit from it. N. lapillus's predation on important habitat forming species plays a key role in the shaping the biodiversity of temperate rocky shores and so these findings have potentially important consequences for the structuring of these communities under near future ocean conditions.

Conclusion

Queirós et al. (2015) found that, considering a large number of ecological processes, N. lapillus populations from highly productive areas may be more likely to be able to compensate for the energetically costly effects of elevated pCO$_2$ and temperature levels. Nevertheless, changes to the shell development, morphology, and composition of juvenile N. lapillus exposed to high pCO$_2$ and temperature conditions observed in this study may lead to higher predation risks. Thus, though some populations may be expected to be more heavily affected by OA and OW than others, considering the low dispersal rates of Nucella due to the direct development, changes in distributional ranges may be foreseen through this enhanced sensitivity of the juvenile stage. Sustainability of populations in regions changing less within the near future and in populations with exceptionally wide genome range could be expected, as some phenotypic plasticity was observed, even within our across-generation study (Lardies et al., 2014; Sunday et al., 2014). However, even sub-lethal effects can affect communities in composition and fitness (Parker et al., 2013), and sub-lethal modifications that may be seen as adaptive, e.g. in behaviour, may be detrimental within a community setting (Queirós et al., 2015). This study highlights that changes in CO$_2$ content and temperature may impact natural populations via effects on early-life stages and developmental plasticity that are not evident in adults, and a large gap remains about how population-level effects of OA and OW may scale to natural systems, in the context of whole communities.

Acknowledgements

Supplementary data

Supplementary material is available at the *ICESJMS* online version of the manuscript.

References

Akaike, H. 1973. Information theory and an extension of the maximum likelihood principle. In 2nd International Symposium on Information Theory, Tsahkadsor, Armenia, USSR, September 2-8, 1971. Ed. by Petrov, B.N. and Csáki, F. Akadémiai Kiadó, Budapest. 267–281.

Barros, P., Sobral, P., Range, P., Chicharo, L., and Matias, D. 2013. Effects of sea-water acidification on fertilization and larval development of the oyster *Crassostrea gigas*. Journal of Experimental Marine Biology and Ecology, 440: 200–206.

Bozhi, J. 2011. Screening of molluscan extrapallial proteins on CaCO3 crystallisation via microfluidics. PhD thesis, University of Glasgow, Glasgow, UK.

Bruker. 2014. DATAVIEWER v1.5.1. Bruker microCT. Kontich, Belgium.

Brusca, R. C., and Brusca, G. J. 2003. Invertebrates. Sinauer Associates, Sunderland, MA, 2nd edn.

Byrne, M., and Przesllawski, R. 2013. Multistressor impacts of warming and acidification of the ocean on marine invertebrates' life histories. Integrative and Comparative Biology, 53: 1–15.

Calosi, P., Rastrick, S. P., Lombardi, C., de Guzman, H. J., Davidson, L., Jahnke, M., Giangrande, A. *et al.* 2013. Adaptation and acclimatization to ocean acidification in marine ectotherms: an in situ transplant experiment with polychaetes at a shallow CO$_2$ vent system. Philosophical Transactions of the Royal Society of London B: Biological Sciences, 368: 1627.

Cascetta, E. 1984. Estimation of trip matrices from traffic counts and survey data: a generalized least squares estimator. Transportation Research, 18: 289–299.

Clarke, K. R. 1993. Non-parametric multivariate analyses of changes in community structure. Australian Journal of Ecology, 18: 117–143.

Clarke, B., and Gorley, R. 2014. Primer 6. PRIMER-E Ltd., Ivybridge, UK.

Cotton, P. A., Rundle, S. D., and Smith, K. E. 2004. Trait compensation in marine Gastropods: Shell shape, avoidance behavior, and susceptibility to predation. Ecology, 85: 1581–1584.

Cusack, M., Perez-Huerta, A., and Dalbeck, P. 2007. Common crystallographic control in calcite biomineralisation of bivalve shells. CrystEngComm, 9: 1215–1218.

Dupont, S., and Thorndyke, M. C. 2009. Impact of CO$_2$-driven ocean acidification on invertebrates early life-history–What we know, what we need to know and what we can do. Biogeosciences Discussions, 6: 3109–3131.

Dupont, S., Dorey, N., Stumpp, M., Melzner, F., and Thorndyke, M. 2013. Long-term and trans-life-cycle effects of exposure to ocean acidification in the green sea urchin *Strongylocentrotus droebachiensis*. Marine Biology, 160: 1835–1843.

Falini, S., Albeck, S., Weiner, S., and Addadi, L. 1996. Control of aragonite polymorphism by mollusk shell macromolecules. Science, 271: 67–69.

Feely, R. A., Sabine, C. L., Lee, K., Berelson, W., Kleypas, J., Fabry, V. J., and Millero, F. J. 2004. Impact of anthropogenic CO$_2$ on the CaCo$_3$ systems in the oceans. Science, 305: 362–366.

FEI. 2013. Amira 5.5. Visualization Sciences Group. FEI Company, Burlington, USA.

Feldkamp, L., Davis, L., and Kress, J. 1984. Practical cone-beam algorithm. Journal of the Optical Society of America, 1: 612–619.

Findlay, H. S., Kendall, M. A., Spicer, J. I., and Widdicombe, S. 2010. Post-larval development of two intertidal barnacles at elevated CO$_2$ and temperature. Marine Biology, 157: 725–735.

Findlay, H. S., Beesley, A., Dashfield, S., Mcneill, C. L., Nunes, J., Queirós, A. M., and Woodward, E. M. S. 2013. UKOA Benthic Consortium, PML intertidal mesocosm experimental environment dataset, (ed Laboratory PM), British Oceanographic Data Centre-Natural Environment Research Council, UK.

Fisher, R. A. 1925. Statistical Methods for Research Workers. Genesis Publishing Pvt Ltd., York University, Toronto, Ontario, Canada.

Fitzer, S. C., Chung, P., Maccherozzi, F., Dhesi, S. S., Kamenos, N. A., Phoenix, V. R., and Cusack, M. 2016. Biomineral shell formation under ocean acidification: a shift from order to chaos. Scientific Reports, 6.

Green, M. A., Jones, M. E., Boudreau, C. L., Moore, R. L., and Westman, B. A. 2004. Dissolution mortality of juvenile bivalves in coastal marine deposits. Journal of Limnology and Oceanography, 49: 727–734.

Guerra-Varela, J., Colson, I., Backeljau, T., Breugelmans, K., Hughes, R. N., and Rolán-Alvarez, E. 2009. The evolutionary mechanism maintaining shell shape and molecular differentiation between two ecotypes of the dogwhelk *Nucella lapillus*. Evolutionary Ecology, 23: 261–280.

Hahn, S., Rodolfo-Metalpa, R., Griesshaber, E., Schmahl, W. W., Buhl, D., Hall-Spencer, J. M., Baggini, C., Fehr, K. T., and Immenhauser, A. 2011. Marine bivalve geochemistry and shell ultrastructures from modern low pH environments. Biogeosciences Discussions, 8: 10351–10388.

Hollander, J., Collyer, M. L., Adams, D. C., and Johannesson, K. 2006. Phenotypic plasticity in two marine snails: constraints superseding life history. The Authors Journal Compilation, 19: 1861–1872.

Hughes, R. N., and Elner, R. 1979. Tactics of a predator, *Carcinus maenas*, and morphological responses of the prey, *Nucella lapillus*. The Journal of Animal Ecology, 48: 65–78.

Hüning, A. K., Melzner, F., Thomsen, J., Gutowska, M. A., Krämer, L., Frickenhaus, S., Rosenstiel, P., *et al.* 2012. Impacts of seawater acidification on mantle gene expression patterns of the Baltic Sea blue mussel: implications for shell formation and energy metabolism. Marine Biology, 160: 1–17.

IPPC. 2014. Summary for Policymakers, In: Climate Change 2014: The Physical Science Basis. Cambridge University Press, Cambridge, United Kingdom and New York, USA.

Klingenberg, C. P. 2011. MorphoJ: an integrated software package for geometric morphometrics. Molecular Ecology Resources, 11: 353–357.

Kruskal, J. B. 1964. Multidimensional scaling by optimizing goodness of fit to a nonmetric hypothesis. Psychometrika, 29: 1–27.

Kurihara, H. 2008. Effects of CO_2-driven ocean acidification on the early developmental stages of invertebrates. Marine Ecology Progress Series, 373: 275–284.

Langerhans, R. B., and Dewitt, T. J. 2002. Plasticity constrained: over-generalized induction cues cause maladaptive phenotypes. Evolutionary Ecology Research, 4: 857–870.

Lardies, M. A., Arias, M. B., Poupin, M. J., Manriquez, P. H., Torres, P. H., Vargas, C. A., Navarro, J. M., and Lagos, N. A. 2014. Differential response to ocean acidification in physiological traits of *Concholepas concholepas* populations. Journal of Sea Research, 90: 127–134.

Marxen, J. C., Prymak, O., Beckmann, F., Neues, F., and Epple, M. 2008. Embryonic shell formation in the snail *Biomphalaria glabrata*: A comparison between scanning electron microscopy (SEM) and synchrotron radiation microcomputer tomography (SRμCT). Journal of Molluscan Studies, 74: 19–25.

Melatunan, S., Calosi, P., Rundle, S. D., Widdicombe, S., and Moody, A. J. 2013. Effects of ocean acidification and elevated temperature in shell plasticity and its energetic basis in an intertidal gastropod. Marine Ecology Progress Series, 472: 155–168.

Melzner, F., Thomsen, J., Koeve, W., Oschlies, A., Gutowska, M. A., Bange, H. W., Hansen, H. P., and Körzinger, A. 2013. Future ocean acidification will be amplified by hypoxia in coastal habitats. Marine Biology, 160: 1875–1888.

Nienhuis, S., Palmer, A. R., and Harley, C. D. G. 2010. Elevated CO_2 affects shell dissolution rate but not calcification rate in a marine snail. Proceedings of the Royal Society of Biological Sciences, 277: 2553–2558.

Órdenes, C., and Antonio, S. 2012. Offspring size, provisioning and performance as a function of maternal investment in direct developing whelks. PhD Thesis, Victoria University of Wellington, New Zealand.

Parker, L. M., Ross, P. M., O'Connor, W. A., Pörtner, H. O., Scanes, E., and Wright, J. M. 2013. Predicting the response of molluscs to the impact of ocean acidification. Biology, 2: 651–692.

Plummer, L. N., and Busenberg, E. 1982. The solubilities of calcite, aragonite and vaterite in CO_2-H_2O solutions between 0-90 °C, and an evaluation of the aqueous model for the system $CaCO_3$-CO_2-H_2O. Geochimica E Cosmochimica Acta, 46: 1011–1040.

Queiroga, H., Costa, R., Leonardo, N., Soares, D., and Clearly, D. F. R. 2011. Morphometric variation in two intertidal littorinoid gastropods. Contributions to Zoology, 80: 201–211.

Queirós, A. M., Fernandes, J. A., Faulwetter, S., Nunes, J., Rastrick, S. P. S., Mieszkowska, N., Artioli, Y., *et al.* 2015. Scaling up experimental ocean acidification and warming research: from individuals to the ecosystem. Global Change Biology, 21: 130–143.

Reed, S. J. B. 2005. Electron Microprobe Analysis and Scanning Electron Microscopy in Geology. Cambridge University Press, Cambridge, UK.

Reusch, T. B. 2014. Climate change in the oceans: evolutionary versus phenotypically plastic responses of marine animals and plants. Evolutionary Applications, 7: 104–122.

Ries, J. B., Cohen, A. L., and McCorkle, D. C. 2009. Marine calcifiers exhibit mixed responses to CO_2-induced ocean acidification. Geology, 37: 1131–1134.

Ries, J. B. 2010. Review: geological and experimental evidence for secular variation in seawater Mg:Ca (calcite-aragonite seas) and its effects on marine biological calcification. Biogeosciences, 7: 2795–2849.

Sanford, E., Gaylord, B., Hettinger, A., Lenz, E. A., Meyer, K., and Hill, T. M. 2014. Ocean acidification increases the vulnerability of native oysters to predation by invasive snails. Proceedings of the Royal Society of Biological Sciences, 281: 1–8.

Selin, N. 2010. Peculiarities of the habitat of Nucella freycineti (Mollusca: Gastropoda) at volcanogenic vent sites. Russian Journal of Marine Biology, 36: 26–33.

Smith, A. M., Key, Jr, M. M., and Gordon, D. P. 2006. Skeletal mineralogy of bryozoans: Taxonomic and temporal patterns. Earth-Science Reviews, 78: 287–306.

Sunday, J. M., Calosi, P., Dupont, S., Munday, P. L., Stillman, J. H., and Reusch, T. B. 2014. Evolution in an acidifying ocean. Trends in Ecology & Evolution, 29: 117–125.

Suzuki, M., and Nagasawa, H. 2013. Shell structures and their formation mechanisms. Canadian Journal of Zoology, 91: 349–366.

Thompson, J. B., Palcoczi, G. T., Kindt, J. H., Michenfelder, M., Smith, B. L., Stucky, G., Morse, D. E., and Hansma, P. K. 2000. Direct observation of the transition from calcite to aragonite growth as induced by abalone shell proteins. Biophysical Journal, 79: 3307–3312.

Thomsen, J., Gutowska, M. A., Saphörster, J., Heinemann, A., Trübenbach, K., Fietzke, J., Hiebenthal, C., Eisenhauer, A., Körzinger, A., Wahl, M., and Melzner, F. 2010. Calcifying invertebrates succeed in a naturally CO_2 enriched coastal habitat but are threatened by high levels of future acidification. Biosciences Discussions, 7: 5119–5156.

Thorson, G. 1950. Reproductive and larval ecology of marine bottom invertebrates. Biology Revisions, 25: 1–45.

Trussel, G. C., Ewanchuck, P. J., and Bertness, M. D. 2003. Trait-mediated effects in rocky intertidal food chains: predator risk cues alter prey feeding rates. Ecology, 84: 629–640.

Turner, L. M., Ricevuto, E., Massa-Gallucci, A., Gambi, M. C., and Calosi, P. 2015. Energy metabolism and cellular homeostasis trade-offs provide the basis for a new type of sensitivity to ocean acidification in a marine polychaete at a high-CO_2 vent: adenylate and phosphagen energy pools versus carbonic anhydrase. Journal of Experimental Biology, 218: 2148–2151.

Vermeij, G. J. 1995. A Natural History of Shells. Princeton University Press, Princeton, New Jersy.

Weiss, I. M., Tuross, N., Addadi, L., and Weiner, S. 2002. Mollusc larval shell formation: Amorphous calcium carbonate is a precursor phase for aragonite. Journal of Experimental Zoology, 293: 478–491.

Widdicombe, S., and Spicer, J. I. 2008. Predicting the impact of ocean acidification on benthic biodiversity: What can animal physiology tell us? Journal of Experimental Marine Biology and Ecology, 366: 187–197.

Wiley, D. F. 2007. Landmark 3.6. Institute of Data Analysis and Visualization (IDAV), University of California, Davis, USA.

Handling editor: Joanna Norkko